J. Fluid Mech. (2004), *vol.* 509, *pp.* 331–351.
DOI: 10.1017/S0022112004008857 Printed in the United Kingdom

The connection between centrifugal instability and Tollmien–Schlichting-like instability for spiral Poiseuille flow

By DAVID L. COTRELL† AND ARNE J. PEARLSTEIN‡

Department of Mechanical and Industrial Engineering, University of Illinois at Urbana-Champaign, 1206 West Green Street, Urbana, IL 61801, USA

(Received 29 April 2003 and in revised form 30 January 2004)

For spiral Poiseuille flow with radius ratio $\eta \equiv R_i/R_o = 0.5$, we have computed complete linear stability boundaries for several values of the rotation rate ratio $\mu \equiv \Omega_o/\Omega_i$, where R_i and R_o are the inner and outer cylinder radii, respectively, and Ω_i and Ω_o are the corresponding (signed) angular speeds. The analysis extends the previous range of Reynolds number Re studied computationally by more than eightyfold, and accounts for arbitrary disturbances of infinitesimal amplitude over the entire range of Re for which spiral Poiseuille flow is stable for some range of the Taylor number Ta. We show how the centrifugally driven instability (beginning with steady or azimuthally travelling-wave bifurcation of circular Couette flow at $Re = 0$ when $\mu < \eta^2$) connects, as conjectured by Reid (1961) in the narrow-gap limit, to a non-axisymmetric Tollmien–Schlichting-like instability of non-rotating annular Poiseuille flow at $Ta = 0$. For $\mu > \eta^2$, we show that there is no instability for $0 \leqslant Re \leqslant Re_{min}$. For $\mu = 0.5$, Re_{min} corresponds to a turning point, beyond which exists a range of Re for which there are two critical values of Ta, with spiral Poiseuille flow being stable below the lower one and above the upper one, and unstable in between. For the special case $\mu = 1$, with the two cylinders having the same angular velocity, Re_{min} corresponds to a vertical asymptote smaller than found by Meseguer & Marques (2002), whose results for $\mu > \eta^2$ fail to account for disturbances with a sufficiently wide range of azimuthal wavenumbers.

1. Introduction

Stability of steady, axisymmetric, incompressible flow driven by differential rotation of coaxial circular cylinders has been investigated extensively since the work of Taylor (1923). Spiral Poiseuille flow (SPF), driven by cylinder rotation and an axial pressure gradient, has been of interest since the experiments of Cornish (1933) and theoretical work of Goldstein (1937), and is important in a number of applications. Papers by Takeuchi & Jankowski (1981) and Ng & Turner (1982) presented the first correct theoretical results concerning the stability of SPF with respect to non-axisymmetric disturbances, and marked the beginning of a more complete understanding of its stability. The best treatments of the stability of this flow are found in their papers, where older work is discussed extensively.

† Present address: NIST, 100 Bureau Drive, Gaithersburg, MD 20899-8910, USA.
‡ Author to whom correspondence should be addressed: ajp@uiuc.edu

For the radius ratio $\eta \equiv R_i/R_o = 0.5$ and rotation rate ratios $\mu \equiv \Omega_o/\Omega_i = -0.5$, 0, and 0.2, Takeuchi & Jankowski investigated the stability of SPF experimentally for $0 \leqslant Re \leqslant 150$ and computationally for $0 \leqslant Re \leqslant 100$, where R_i and R_o are the radii of the inner and outer cylinders whose respective constant (signed) angular speeds are Ω_i and Ω_o, the Reynolds number Re is defined by $\overline{V}_Z (R_o - R_i)/\nu$, and $\overline{V}_Z$ and ν are the mean axial speed of the base flow and the kinematic viscosity, respectively. They found that the critical value of the Taylor number $Ta \equiv \Omega_i (R_o - R_i)^2/\nu$ is strongly affected by Re and μ. For $\mu = 0$ and 0.2, Ta_{crit} initially increases as Re increases from zero, with the critical disturbance remaining axisymmetric. This stabilization continues until a (globally) maximum Ta_{crit} is reached at some Re. Beyond the maximum, for $\mu = 0$, Ta_{crit} decreases but still exceeds its $Re = 0$ value over the entire Re range considered by Takeuchi & Jankowski, while for $\mu = 0.2$, Ta_{crit} falls below its $Re = 0$ value. For $\mu = -0.5$, Ta_{crit} decreases as Re increases from zero (i.e. SPF is destabilized by sufficiently slow axial flow) with a critical azimuthal wavenumber (m_{crit}) of 1, and continues to decrease until a local minimum is reached. As Re increases further, the critical Ta increases until m_{crit} changes to 2, beyond which point Ta_{crit} decreases with Re until reaching a second (lower) local minimum. For still larger Re, Ta_{crit} increases monotonically with Re over the range considered by Takeuchi & Jankowski. For $\mu = 0$ and 0.2, experimental and computational results are in excellent agreement for $Re \leqslant 40$, with experimental values of Ta_{crit} at higher Re exceeding computed values to an extent that increases with Re. (Use of the symbols Re and Ta in this paper to refer to Reynolds and Taylor numbers defined differently by others implies conversion to our definitions.) For $\mu = -0.5$, the experimental Ta_{crit} exceeds the computed value over the entire range of Re. For each μ, however, the experimental and computed stability boundaries are qualitatively similar.

In contemporaneous work, Ng & Turner (1982) performed computations for $\eta = 0.77$ and 0.95, with $\mu = 0$. They considered axisymmetric and non-axisymmetric disturbances over $0 \leqslant Re \leqslant 6000$ for both radius ratios, and axisymmetric disturbances over $6000 < Re \leqslant 7739.5$ for $\eta = 0.95$. For both radius ratios, Ta_{crit} was found to increase as Re increases from zero, ultimately reaching a broad plateau. For $\eta = 0.95$, the Ta at which SPF becomes unstable with respect to axisymmetric disturbances decreases rapidly beyond $Re = 6000$. Their results agree well with the $\mu = 0$ experimental results of Mavec (1973) up to $Re = 400$ for $\eta = 0.77$ and Snyder (1962, 1965) up to $Re = 200$ for $\eta \approx 0.95$.

Since the investigations of Takeuchi & Jankowski and Ng & Turner, work on SPF has focused on its use at low Re as an open system to study convective and absolute instabilities and noise amplification and noise-sustained structures (Babcock, Ahlers & Cannell 1991, 1994; Babcock, Cannell & Ahlers 1992; Lücke & Recktenwald 1993; Recktenwald, Lücke & Müller 1993; Tsameret & Steinberg 1991*a*, *b*, 1994a; Swift, Babcock & Hohenberg 1994; Tsameret, Goldner & Steinberg 1994), pattern formation and supercritical mode structure (Bühler & Polifke 1990; Raffaï & Laure 1993; Tsameret & Steinberg 1994*b*; Büchel *et al.* 1996; Wereley & Lueptow 1999; Moser *et al.* 2000; Moser, Raguin & Georgiadis 2001; Pinter, Lücke & Hoffmann 2003), and secondary instabilities (Lueptow, Docter & Min 1992). Closely related filtration flows in which one cylinder is porous (Min & Lueptow 1994; Kolyshkin & Vaillancourt 1997; Johnson & Lueptow 1997), and flows in which the axial velocity component is time-periodic (Hu & Kelly 1995; Weisberg, Kevrekidis & Smits 1997; Marques & Lopez 2000) have also attracted interest.

More recently, Meseguer & Marques (2002) reported linear stability computations for $\eta = 0.5$. For $\mu \neq 1$, they considered an Re range ($0 \leqslant Re \leqslant 125$) similar to those

considered by Takeuchi & Jankowski, while computations for $\mu = 1$ extended up to $Re = 4000$. Their $\mu = 0$ results were indistinguishable from those of Takeuchi & Jankowski, while no comparison was made to experiments or computations of Takeuchi & Jankowski for $\mu = -0.5$ or 0.2, or to computations of Joseph & Munson (1970) for $\mu = 1$.

Despite considerable interest in SPF, the complete linear stability boundary in, say, the (Ta, Re)-plane, has not been determined for any combination of the remaining parameters. To the best of our knowledge, the only computational work on the stability of SPF for any combination of μ and η since the work of Takeuchi & Jankowski and Ng & Turner is that of Recktenwald *et al.* (1993) and Pinter *et al.* (2003), limited to the range $0 \leqslant Re \leqslant 20$, and that of Meseguer & Marques (2002).

Since Reid (1961) conjectured, in the narrow-gap context, that low-Re stabilization of SPF by axial flow must give way to an instability of Tollmien–Schlichting (TS) type at higher Re, that connection has been made only for $\mu = 0$ and $\eta = 0.95$, and then only for axisymmetric disturbances (Ng & Turner 1982). As shown by Cotrell, Rani & Pearlstein (2004, hereinafter referred to as Part 2), transition from a centrifugal instability to a TS-like instability occurs at $Re = 7716$ for this μ and η, with non-zero azimuthal wavenumbers for both modes, in a range ($6000 \leqslant Re \leqslant 7739.5$) in which the work of Ng & Turner was restricted to axisymmetric disturbances.

Here, we report complete SPF stability boundaries for $\eta = 0.5$, the radius ratio considered by Takeuchi & Jankowski and Meseguer & Marques (2002). The results account for arbitrary infinitesimal disturbances and extend the range of Re studied by more than eightyfold, covering the entire range of Re for which SPF is linearly stable for some range of Ta. We consider $\mu = 0$, in which case the outer cylinder is fixed, as well as $\mu > 0$ and $\mu < 0$ (co- and counter-rotating cylinders, respectively). For $\mu < \eta^2$, we connect the centrifugally driven instability at $Re = 0$ to the non-axisymmetric TS-like instability of annular Poiseuille flow (Mahadevan & Lilley 1977; Sadeghi & Higgins 1991) at $Ta = 0$. For $\mu > \eta^2$, for which Synge (1938) showed that no linear instability is possible for $Re = 0$, we demonstrate the exsistence of a turning point for $\mu \neq 1$ and a vertical asymptote for $\mu = 1$.

The paper is organized as follows. In § 2, we briefly present the formulation. The numerical approach is described in § 3. Complete stability boundaries for $\eta = 0.5$ are presented for $\mu = 0$ (§ 4.1), $\mu > 0$ (§ 4.2), and $\mu < 0$ (§ 4.3). This is followed by a discussion in § 5, and some conclusions in § 6. Results for the larger values of η pertinent to most experiments are reported in Part 2, where extensive comparison is made to experimental data for a wide range of Reynolds numbers and rotation rate ratios.

2. Formulation

For a constant-property fluid, we consider flow between concentric circular cylinders driven jointly by a constant axial pressure gradient and rotation of one or both cylinders. We choose an inertial frame in which the cylinders have no axial velocity. The governing equations are non-dimensionalized using the dimensionless radial coordinate $r = R/(R_o - R_i)$, axial coordinate $z = Z/(R_o - R_i)$, time $\tau = t\overline{V}_Z/(R_o - R_i)$, velocity $\boldsymbol{v} = \boldsymbol{V}/\overline{V}_Z$, and pressure $p = P/(\rho\overline{V}_Z^2)$ employed by Takeuchi & Jankowski.

The steady, axisymmetric, fully developed base flow satisfying no-slip conditions on the rigid inner and outer walls at $r = \eta/(1-\eta)$ and $1/(1-\eta)$, respectively, is

$$v_{rb} = 0, \tag{2.1a}$$

$$v_{\theta b} = \frac{Ta}{Re}\left[\frac{r(\mu-\eta^2)}{(1-\eta^2)} + \frac{\eta^2(1-\mu)}{r(1-\eta)^3(1+\eta)}\right], \tag{2.1b}$$

$$v_{zb} = 2\left[\frac{[1-r^2(1-\eta)^2]\ln\eta - (1-\eta^2)\ln[r(1-\eta)]}{1-\eta^2+(1+\eta^2)\ln\eta}\right]. \tag{2.1c}$$

With this non-dimensionalization, the base flow for fixed η consists of an axial component whose profile and magnitude are constant, and an azimuthal component whose profile depends on μ and whose magnitude is proportional to Ta/Re.

The disturbance velocity and pressure fields (denoted by $'$) in normal mode form are

$$\begin{bmatrix} \boldsymbol{v}'(r,\theta,z,\tau) \\ p'(r,\theta,z,\tau) \end{bmatrix} = \begin{bmatrix} \tilde{\boldsymbol{v}}(r) \\ \tilde{p}(r) \end{bmatrix} \exp\left[\mathrm{i}\,(kz+m\theta)+\sigma\tau\right] \tag{2.2}$$

where k, m, and σ are the axial wavenumber, azimuthal wavenumber, and temporal eigenvalue, respectively. We take k to be real and σ to be complex. Neglecting nonlinear terms, we obtain a homogeneous linear ordinary differential equation system in the radial coordinate for the disturbance velocity components and pressure, equivalent to equations (6*a–d*) of Takeuchi & Jankowski.

Stability of SPF has been studied using three different parametrizations. Takeuchi & Jankowski and Ng & Turner reported critical Taylor numbers versus Re for selected μ. Snyder (1965) and Mavec (1973) presented critical values of an inner-cylinder Taylor number versus an outer-cylinder Taylor number for selected Re. Finally, Meseguer & Marques (2002) presented critical inner-cylinder Taylor numbers versus Re for selected values of an outer-cylinder Taylor number. For the parametrization of Takeuchi & Jankowski and Ng & Turner chosen here, the profiles of the azimuthal and axial velocity components are independent of Ta and Re, allowing centrifugal and axial shear effects to be assessed independently of profile changes at fixed μ, as in the limiting cases of annular Poiseuille flow (no rotation) and circular Couette flow (no axial pressure variation).

3. Numerical approach

We discretize the disturbance equations by collocation, using M_p and M_p-1 Chebyshev polynomials to represent the disturbance velocity components and pressure, respectively. The momentum and continuity equations are collocated at M_p-2 interior Gauss–Lobatto points and M_p-1 interior Gauss points, respectively, and the boundary conditions are satisfied explicitly, giving a generalized matrix eigenvalue problem

$$\boldsymbol{A}\boldsymbol{x} = \sigma\boldsymbol{B}\boldsymbol{x}, \tag{3.1}$$

of dimension $4M_p-1$, whose temporal eigenvalues $\sigma=\sigma_r+\mathrm{i}\sigma_i$ are found using LAPACK.

For given Re, μ, and η, we seek critical values of Ta, for which at least one temporal eigenvalue has $\sigma_r=0$ for some m and k, and all other σ lie in the left half-plane for all m and k. As discussed by Takeuchi & Jankowski, Ng & Turner, and Meseguer & Marques (2002), analysis can be restricted to $k\geqslant 0$ without loss of generality.

To compute critical values of Ta, we begin with $153\leqslant M_k\leqslant 202$ discrete axial wavenumbers non-uniformly distributed over $0<k\leqslant 100$. For each m considered (*vide infra*), we do 'axial wavenumber traverses' at fixed Ta, until we locate a value (Ta_s) stable at each of the M_k wavenumbers and another (Ta_u) unstable for at least one k. For each of Ta_s and Ta_u, we identify the k_j, among the M_k considered,

at which σ_r assumes its maximum, and fit a quadratic through the points (σ_r, k), with $k = k_{j-1}$, k_j, and k_{j+1}. Differentiating, we estimate values of k maximizing σ_r at Ta_s and Ta_u, and use this process to iteratively refine k at each Ta until $| 1 - \sigma_{r,n+1}^{max}/\sigma_{r,n}^{max} | < \epsilon_1$. Once maximum values of σ_r (negative for Ta_s and positive for Ta_u) and the corresponding k are found, secant iteration between Ta_s and Ta_u is used to estimate a new Ta_1 at which σ_r^{max} vanishes. A wavenumber traverse at this Ta gives the sign of σ_r^{max}, which determines whether Ta_s or Ta_u is replaced. Secant iteration is continued until $| 1 - Ta_{l+1}/Ta_l | < \epsilon_2$. (Requiring convergence of $| 1 - Ta_s/Ta_u |$ gave indistinguishable stability boundaries.) At this juncture, for each m we have one or more extremal values of Ta and associated values of k. For each m, such a (k, Ta) pair corresponds to an extremum on a (k, Ta) neutral curve (i.e. a curve dividing portions of the (k, Ta)-plane in which no temporal eigenvalue lies in the right half-plane (RHP), from portions in which one or more eigenvalues lie in the RHP). The critical azimuthal wavenumber m_{crit} is determined as follows. Except when $\mu \geqslant \eta^2$, each stability boundary begins at $Re = 0$, where m_{crit} is easily found (DiPrima & Swinney 1985). A range of m, typically of width 6–20, centred about this initial m, is considered, and m_{crit} is determined as the value for which no eigenvalues lie in the RHP for any combination of m and k at the extremal Ta. The corresponding critical axial wavenumber and wave speed are denoted by k_{crit} and $c_{crit} = -\sigma_{i,crit}/k_{crit}$. For $Re > 0$, the initial estimate of m_{crit} is obtained from results at nearby values of Re.

For $\mu > \eta^2$, the procedure is identical, except that m_{crit} cannot be estimated from m_{crit} for circular Couette flow at $Re = 0$, which is stable with respect to all infinitesimal disturbances. Instead, we first find a (positive) Re for which one or more unstable values of Ta exist for some m. We then compute extremal values of Ta for each m in a range centred about $m = 0$. After m_{crit} is found for this initial Re, we use it as the starting point to compute the remainder of the stability boundary as described above.

For each μ, we examined a range of m (sometimes not identical to the initial range), sufficiently large that it was clear that Ta_{crit} varies monotonically for m beyond its limits. As shown in § 4, $m_{crit} \geqslant 0$ unless $\mu > \eta^2$. Nonetheless, for each $\mu < \eta^2$, spot checks were performed for $m < 0$, and in no case was a neutral Ta found below the Ta_{crit} value computed for $m \geqslant 0$, consistent with the results of Takeuchi & Jankowski. The importance of considering a sufficient range of m cannot be overemphasized (see § 4.2).

For given μ, an upper limit on the range of k_{crit} was estimated by computing critical values of Ta, m, and k at several (5–10) Re values distributed over $0 \leqslant Re \leqslant Re_{AP}$ using a very large range of k, where Re_{AP} is the critical Re for (non-rotating) annular Poiseuille flow. The values of k_{crit} were used to choose the discrete set of k used at intermediate Re for given μ. The resulting continuous dependence of Ta_{crit} on Re strongly suggests that this approach is a correct one and has been correctly applied.

As shown in § 4.2, there are values of μ for which ranges of Re exist in which there are two or three critical Ta. In these cases, closed disconnected neutral curves (cf. Lopez, Romero & Pearlstein 1990 and references cited therein) exist whose extrema must be found. While techniques developed to do this systematically for stability problems in which the constant-coefficient differential equations allow closed-form solution (Terrones & Pearlstein 1989) can be generalized to systems requiring approximate spatial discretization, rapid growth of computational complexity with matrix size makes that approach impractical for the level of resolution required for most non-zero base flows. Thus, after first recognizing the existence of an Re range in which multiplicity occurs, we used the procedure described above with several pairs of initial Ta values. In each case, the topology of the computed stability boundary was consistent with all critical values having been found.

M_p	γ	M_p	γ
10	1.78×10^{-2}	20	5.63×10^{-7}
12	7.77×10^{-3}	22	1.11×10^{-7}
14	1.24×10^{-3}	24	1.5×10^{-8}
16	8.06×10^{-5}	26	1.0×10^{-9}
18	1.39×10^{-6}		

TABLE 1. Discretization convergence $\gamma = |Ta_{crit,M_p} - Ta_{crit,M_{p,max}}|$ for $Re = 100$, $\mu = 0$, $\eta = 0.5$, and $M_{p,max} = 40$.

To validate the code, we compared our results to previous SPF stability calculations. For all values of Re and μ shown in table 1 of Takeuchi & Jankowski, our computed values of Ta_{crit}, m_{crit}, and k_{crit} agree with theirs to the number of significant figures shown by them. For $\eta = 0.77$, our results agree with those tabulated by Ng & Turner over the entire Re range they considered ($0 \leqslant Re \leqslant 6000$), except for m_{crit} and c_{crit} at $Re = 300$ and 500. For these two cases, our m_{crit} values are smaller by 1. The Ta_{crit} values agree to within one part in 50 000, and the k_{crit} values differ by less than 0.1%, even at the two Re values at which m_{crit} is discrepant. For $\eta = 0.95$, our Ta_{crit} values agree to at least three significant figures with those of Ng & Turner over $0 \leqslant Re \leqslant 6000$. Agreement is considerably better except at $Re = 10$, 100, and 2000, where our m_{crit} values are 1 larger, 1 smaller, and 1 larger, respectively, and there are small differences in k_{crit}. For $\eta = 0.95$, larger differences over the range $6000 < Re < 7739.5$ between the results of Ng & Turner for axisymmetric disturbances and ours for arbitrary disturbances are discussed in Part 2. Comparison to the low-Re results of Recktenwald *et al.* (1993) for $\mu = 0$ is also excellent. For $\eta = 0.5$, the root-mean-square (r.m.s.) difference between our computed Ta_{crit} values at $Re = 1, 2, \ldots, 20$ and those corresponding to the fitted form of Recktenwald *et al.* is 1.2×10^{-3}, with $Ta_{crit} \geqslant 60$ over that range. The r.m.s. differences between k_{crit} and c_{crit} values are 1.7×10^{-5} and 1.6×10^{-4}, respectively, compared to k_{crit} and c_{crit} on the order of 3 and 1, respectively. Comparison to work for annular Poiseuille flow shows excellent agreement between our critical Re values and the tabulated results of Sadeghi & Higgins (1991) (less than 1% difference for $\eta = 0.5$), and the graphical results of Mahadevan & Lilley (1977) and Garg (1980) at smaller η.

To ensure that critical values are fully resolved, we checked convergence for a range of Re at each μ. In general, the number of terms M_p ensuring a specified accuracy for a given Ta increases with Re. Table 1 shows, for $\mu = 0$ and $Re = 100$, the magnitude γ of the difference between Ta values determined using M_p and $M_{p,max}$ terms, where $M_{p,max}$ is the largest M_p used in this case. We have used $\epsilon_1 = 10^{-6}$, $\epsilon_2 = 2 \times 10^{-7}$, and achieved convergence with $M_{p,max} \leqslant 40$ for each combination of Re, μ, and η. We believe that the small differences between our results and those of Ng & Turner in the few cases cited above are due to our use of somewhat more stringent convergence criteria, parametrized by M_p (spatial resolution), ϵ_1 (axial wavenumber iteration), and ϵ_2 (Ta iteration).

4. Results

We report complete linear stability boundaries in the (Re, Ta)-plane, accounting for three-dimensional disturbances, for $\eta = 0.5$ at each μ considered by Takeuchi & Jankowski, as well as at $\mu = 0.5$. The results cover the range from $Re = 0$ (the

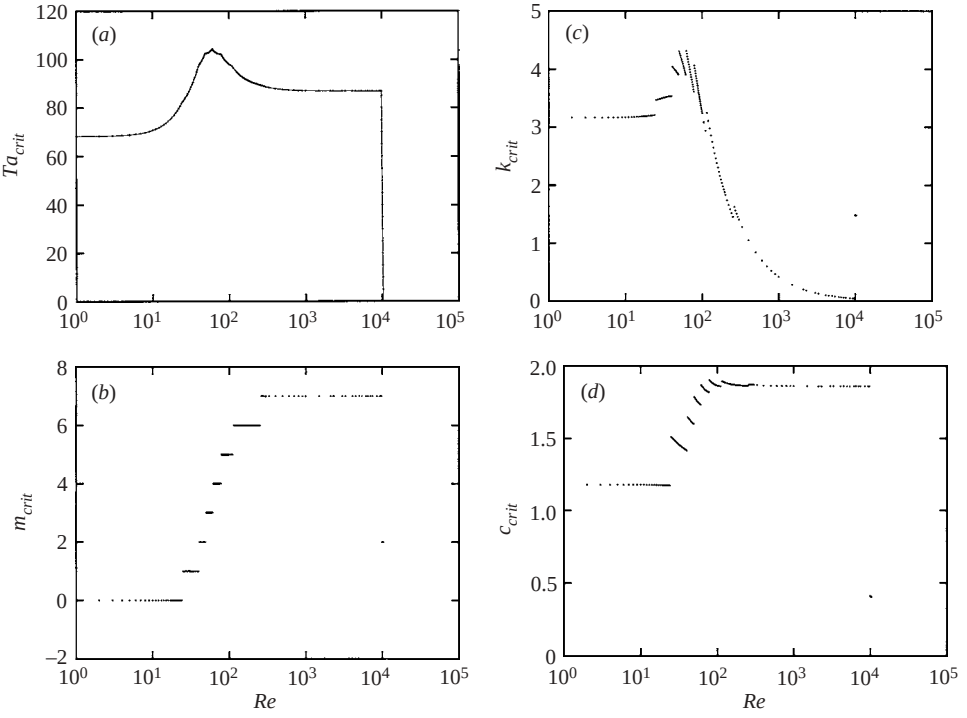

FIGURE 1. For $\mu = 0$ and $\eta = 0.5$: (*a*) critical Ta, (*b*) critical m, (*c*) critical k, (*d*) critical c, versus Re.

Taylor–Couette limit) to Re_{AP} (the μ-independent Re beyond which the base flow is unstable for every Ta, corresponding to onset of TS-like instability in the non-rotating annular Poiseuille flow).

4.1. *Non-rotating outer cylinder* ($\mu = 0$)

Here, we briefly review the $\mu = 0$ results for $0 \leqslant Re \leqslant 150$, and then focus on larger Re up to $Re_{AP} = 10\,359$.

At $Re = 0$, Ta_{crit} is 68.19 (DiPrima & Swinney 1985), corresponding to onset of centrifugal instability and Taylor vortices. For small Re, the flow is stabilized by increasing axial flow (see figure 1*a*), with Ta_{crit} reaching a maximum of about 104.4 near $Re \approx 61$, as shown by Takeuchi & Jankowski. The scalloped stability boundary is associated with the 'stair-step' behaviour of m_{crit}, as shown in figure 1(*b*) and discussed by Takeuchi & Jankowski. As noted by those authors, shear generally destabilizes SPF for $61 \leqslant Re \leqslant 150$. Figure 1(*a*) shows that this destabilization continues to about $Re = 400$.

On a plateau over the range $400 < Re < Re^* = 9916$, Ta_{crit} (≈ 88) is greater than its non-rotating value of 68.19. The existence of this plateau indicates that the magnitude of the axial component of the base flow does not significantly affect the centrifugal instability in this range of Re. At Re^*, Ta_{crit} begins a precipitous fall, corresponding to transition from centrifugal instability to a parallel shear instability (associated with a critical layer) of TS-type. While the slope of Ta_{crit} vs. Re is discontinuous at Re^*, Ta_{crit} is a continuous function of Re. The flow is unstable for all Ta beyond $Re_{AP} = 10\,359$, a value agreeing with the graphical results of Mahadevan & Lilley

(1977) and Garg (1980) for non-rotating annular Poiseuille flow as well as they can be read.

Figure 1(*b*) shows that m_{crit} increases by one unit at each of seven Reynolds numbers in the range $0 < Re < 270$. (The jump of 2 in m_{crit} between $Re = 40$ and 50 shown in table 1 of Takeuchi & Jankowski is clearly due to the gap between consecutive Re values.) The critical azimuthal wavenumber drops directly from 7 to 2 as Re passes through Re^*. On the TS-like branch ($Re^* < Re \leqslant Re_{AP}$), $m_{crit} = 2$.

Figures 1(*b*) and 1(*c*) show that the discontinuous dependence of k_{crit} on Re is associated with jumps in m_{crit}. For $Re < 41$, $m_{crit} = 0$ or 1 and k_{crit} increases monotonically with Re, while for $Re \geqslant 41$, k_{crit} decreases monotonically over each constant-m_{crit} range of Re. For $Re \leqslant Re_{AP}$, k_{crit} increases discontinuously at each m_{crit} jump, leading to the 'wavenumber fan' shown. For $260 \leqslant Re \leqslant Re^*$, for which $m_{crit} = 7$, k_{crit} decreases, nearly inversely with Re, to very small values ($k_{crit} = 0.0422$ at $Re = 9914$), consistent with visualization of the secondary flow (Nagib 1972; Joseph 1976). As Re passes through Re^*, k_{crit} increases more than thirtyfold. Between Re^* and Re_{AP} on the TS-like branch, k_{crit} varies between 1.481 and 1.479, reflecting the fact that the TS-like instability is driven by axial shear, and that Re changes by only about 4% on that branch.

Figure 1(*d*) shows the piecewise-continuous dependence of c_{crit} on Re. For small Re, c_{crit} is essentially constant (see figure 1*d*), implying that the dimensional frequency vanishes linearly as $\overline{V}_Z \to 0$, consistent with the well-known result for Taylor–Couette instability with $\mu = 0$. Since $m_{crit} = 0$ for small Re, this corresponds to transition from a steady axisymmetric disturbance flow at $Re = 0$ to a time-periodic axisymmetric flow at $Re > 0$, as Taylor-like vortices propagate axially. As with k_{crit}, discontinuities in c_{crit} at higher Re correspond to jumps in m_{crit}. For $0 < Re < 260$, c_{crit} decreases monotonically over each range of Re for which m_{crit} remains unchanged. Over $260 < Re < Re^*$, for which $m_{crit} = 7$, $c_{crit} \approx 1.86$. As Re increases beyond Re^*, c_{crit} discontinuously drops to values characteristic of instability for annular Poiseuille flow, with the dimensionless wave speed values suggesting existence of a critical layer for $Re^* < Re < Re_{AP}$.

4.2. *Co-rotating outer cylinder* ($\mu > 0$)

Takeuchi & Jankowski investigated the co-rotating case $\mu = 0.2$ over the ranges $0 \leqslant Re \leqslant 100$ computationally, and $0 \leqslant Re \leqslant 150$ experimentally. We have computed the complete linear stability boundary partially determined by those authors, extending Re to Re_{AP}. We also present results for $\mu = 0.5$, beyond the Rayleigh criterion. Finally, we reconsider the results of Meseguer & Marques (2002) for $\mu > 0$.

The stability boundary for $\mu = 0.2$ (not shown) is somewhat similar to that for $\mu = 0$ (figure 1*a*). At $Re = 0$, we find $Ta_{crit} = 124.7$. The critical Ta increases to a maximum of about 170 near $Re = 36$. For larger Re, Ta_{crit} decreases monotonically, first to a broad plateau ($Ta_{crit} \approx 79$), and then, beginning at $Re^* = 9979$, plunges to zero at $Re_{AP} = 10\,359$. In addition to the scalloping associated with stepwise variation in m_{crit} and the precipitous decline in Ta_{crit} associated with a TS-like instability, the stability boundary shows that the high-Re plateau lies at a lower Ta_{crit} than the $Re = 0$ limit, so that for $64 \leqslant Re \leqslant Re^*$, shear destabilizes SPF relative to the $Re = 0$ situation. This differs from the $\mu = 0$ case discussed above, and is consistent with the work of Takeuchi & Jankowski, whose results do not extend to the plateau region. This trend is opposite to that predicted for $\mu = 0$, where Ta_{crit} was higher on the high-Re plateau than at $Re = 0$. The dependence of m_{crit} on Re is similar to that for $\mu = 0$, with the largest value (on the plateau) being 6 rather than 7. Variation of k_{crit} and c_{crit} with Re is also similar to that for $\mu = 0$.

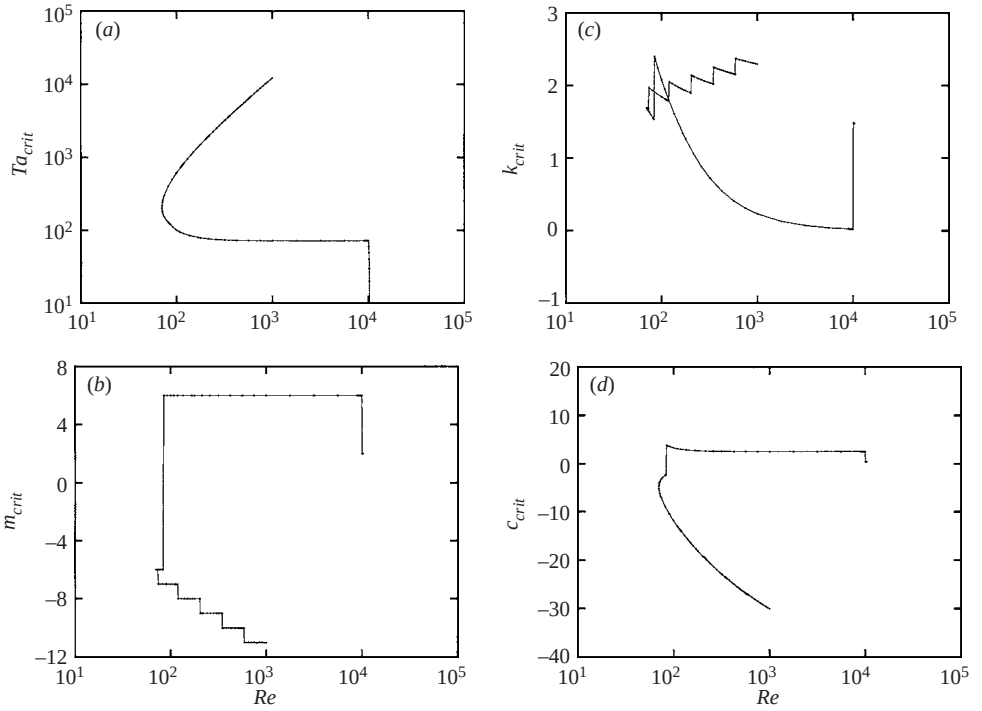

FIGURE 2. For $\mu = 0.5$ and $\eta = 0.5$: (*a*) critical *Ta*, (*b*) critical *m*, (*c*) critical *k*, (*d*) critical *c*, versus *Re*.

Figure 2(*a–d*) shows the stability boundary, m_{crit}, k_{crit}, and c_{crit} for $\mu = 0.5$. Since $\mu > \eta^2$, the viscous extension of the Rayleigh criterion (Synge 1938) shows that no linear instability is possible for $Re = 0$. In fact, in this case figure 2(*a*) shows that SPF is linearly stable up to a turning point at $Re_{min} = 70.2$, beyond which Ta_{crit} increases rapidly with *Re* on one branch of the stability boundary, while on the other Ta_{crit} decreases to a plateau ($Ta \approx 70$), and then falls precipitously at $Re^* = 10\,049$, reaching zero at $Re_{AP} = 10\,359$. Thus, for $Re_{min} \leqslant Re \leqslant Re_{AP}$, SPF is linearly stable below the lower critical *Ta* and above the upper critical value, and unstable in between. (Computation on the upper branch is difficult beyond $Re = 1000$ due to rapid growth in the number of expansion functions needed to maintain adequate resolution.)

Multi-valuedness of the stability boundary in figure 2(*a*) is associated with disconnected neutral curves in the (k, Ta)-plane for $Re > Re_{min}$. Consistent with the work of Synge, for $\mu = 0.5$ there are no neutral curves if $Re < Re_{min}$. Figure 3 shows that for $Re = 100$ the neutral curves for $-14 \leqslant m \leqslant -3$ and $3 \leqslant m \leqslant 9$ are closed, and each extends over only a finite *Ta* range. At Re_{min}, the first neutral curve (for $m = -6$; see figure 2*b*) appears as a point, and grows as *Re* increases. For each *m*, the process is essentially identical to the appearance of closed disconnected neutral curves in buoyancy-driven stability problems (Pearlstein 1981; Pearlstein, Harris & Terrones 1989; Terrones & Pearlstein 1989; Lopez *et al.* 1990; Ali & Weidman 1990), and as in those cases, a multi-valued stability boundary (figure 2*a*) results. Between $Re = Re_{min}$ and $Re = 100$, the other neutral curves shown in figure 3 first appear as points, and grow as *Re* increases. The $Re = 100$ neutral curves were determined by a grid search for instability in the (k, Ta)-plane, using *k* and *Ta* increments of 0.01 and

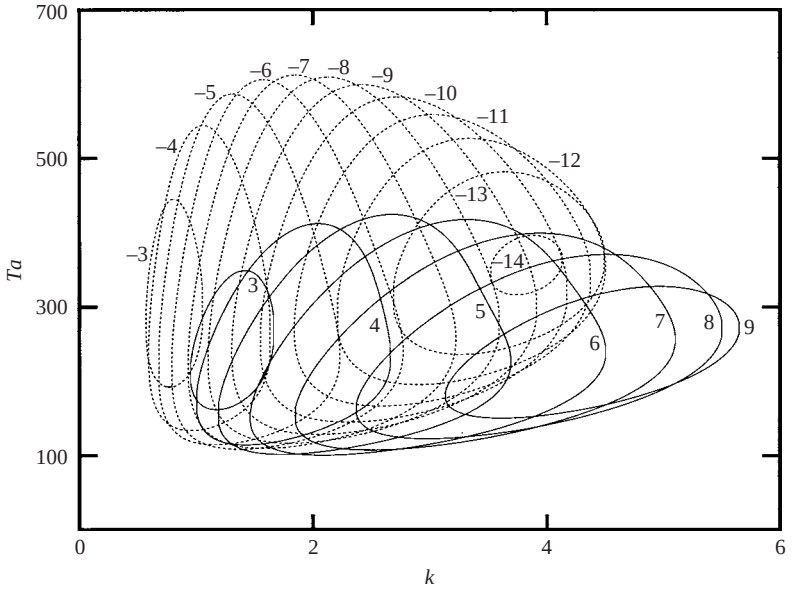

FIGURE 3. Neutral curves for $Re = 100$ and $\mu = \eta = 0.5$, corresponding to azimuthal wavenumbers in the ranges $-14 \leqslant m \leqslant -3$ (dashed) and $3 \leqslant m \leqslant 9$ (solid).

10, respectively. At $Re = 100$, these are the only neutral curves found for $-20 \leqslant m \leqslant 11$ over the ranges $0.1 \leqslant k \leqslant 10$ and $0 \leqslant Ta \leqslant 1000$.

As shown in figure 2(b), $m_{crit} = 2$ on the TS-like branch, and jumps to 6 as Re decreases through Re^*. It remains 6 as Re decreases further on the lower branch of the stability boundary until jumping to -6 at $Re = 84$, just short of the turning point. The value of m_{crit} is -6 through the turning point at $Re = 70.2$, with a jump to -7 at $Re = 73$ on the upper branch, followed by unit decreases as Re increases. (Vertical line segments with no filled circles between their endpoints in figure 2(b–d) denote jump discontinuities in m_{crit}, k_{crit}, and c_{crit}, and are provided to clarify variation of these quantities along the stability boundary.) We find no Re for which an axisymmetric disturbance is critical.

Figure 2(c) shows that k_{crit} is again about 1.48 on the TS-like branch, and jumps to 0.026 as Re decreases through Re^*. As Re decreases further on the upper branch of the stability boundary, k_{crit} increases roughly like $1/Re$ ($204 \leqslant k_{crit} Re \leqslant 235$ for $8.6 \leqslant Re \leqslant 9000$), until m_{crit} jumps from 6 to -6, at which point k_{crit} jumps from 2.41 to 1.53. On the $m_{crit} = -6$ portion of the lower branch of the stability boundary, k_{crit} increases as the turning point at $Re = 70.2$ is approached, and continues to increase on the upper branch to 1.70 at $Re = 70.3$. Beyond that point, k_{crit} decreases as Re increases on the $m_{crit} = -6$ portion of the upper branch, reaching 1.69 at $Re = 72.8$. At that point, m_{crit} decreases to -7, and k_{crit} jumps to 1.97 before decreasing monotonically to 1.79 at $Re = 118.6$. As Re increases further, k_{crit} exhibits 'fan-like' behaviour, decreasing monotonically as Re increases for each m_{crit}, and increasing discontinuously at each jump decrease of m_{crit}.

On the TS-like branch, c_{crit} varies between 0.40 and 0.41 (figure 2d), and jumps discontinuously to about 2.50 as Re decreases through Re^*. It remains nearly constant on the plateau, increasing slightly as the transition from $m_{crit} = 6$ to -6 is approached. At that transition, c_{crit} discontinuously jumps to negative values, and decreases

		$-\infty < m < \infty$			$m \geqslant 0$		
(*a*)	Ta	Re_{crit}	k_{crit}	m_{crit}	$Re_{m\geqslant 0}$	$k_{m\geqslant 0}$	$m_{m\geqslant 0}$
	100	115.5	0.9839	−6	151.1	1.016	5
	225	87.65	0.8087	−8	103.2	0.8844	6
	300	85.18	0.6265	−8	99.97	0.6968	6
	400	83.88	0.4778	−8	98.23	0.5371	6
	1000	82.55	0.1944	−8	96.41	0.2201	6
	2000	82.36	0.09740	−8	96.16	0.1108	6
		$-\infty < m < \infty$			$m \geqslant 0$		
(*b*)	Re	Ta_{crit}	k_{crit}	m_{crit}	$Ta_{m\geqslant 0}$	$k_{m\geqslant 0}$	$m_{m\geqslant 0}$
	150	79.82	0.9200	−6	100.7	1.018	5
	200	71.52	0.7550	−6	84.51	0.8695	5
	300	66.82	0.5310	−6	76.16	0.6257	5
	500	64.70	0.3263	−6	72.55	0.3891	5
	1000	63.86	0.1640	−6	71.13	0.1975	5

TABLE 2. (*a*) Minimum neutral values of Re, and (*b*) minimum neutral values of Ta (and corresponding values of k and m) for different ranges of m at selected Re with $\mu = 1$ and $\eta = 0.5$.

monotonically through the turning point and beyond. The small discontinuities in c_{crit} at the m_{crit} jumps on the upper branch are indiscernible in figure 2(*d*). We note that the negative values of c_{crit} on the upper branch and on part of the lower branch of the stability boundary correspond to disturbances propagating upstream against the axial flow, and that c_{crit} does not vanish at any point on the stability boundary. This point is discussed in § 5.6.

The special case $\mu = 1$, corresponding to a base flow with uniform angular velocity, has been considered by Meseguer & Marques (2002). Their figure 13 shows the critical Ta approaching 70.69 (with $m_{crit} = 5$) at high Re, and the critical Re approaching a vertical asymptote at 96.14 (with $m_{crit} = 6$) at high Ta. The latter result disagrees with the computations of Joseph & Munson (1970), who showed that for $\eta = 0.5$ and $\mu = 1$, $2Re_{crit} \approx 165$ (Joseph 1976, figure 46.1) in the $Ta \to \infty$ limit.

The results presented in tables 2(*a*) and 2(*b*) show that the asymptotes reported by Meseguer & Marques (2002) are incorrect, with the correct horizontal and vertical asymptotes being near $Ta_{crit} = 63.86$ (with $m_{crit} = -6$) and $Re_{crit} = 82.33$ ($m_{crit} = -8$), respectively, the latter value being very close to that reported by Joseph (1976). Tables 2(*a*) and 2(*b*) show that the values reported by Meseguer & Marques (2002) correspond very closely to the smallest Ta (71.13) and Re (96.16) obtained when only positive values of m are considered, providing convincing evidence that those authors considered an insufficient range of azimuthal wavenumbers.

4.3. *Counter-rotating outer cylinder* ($\mu < 0$)

For $\mu = -0.5$, figure 4(*a*) shows the complete stability boundary partially determined by Takeuchi & Jankowski (1981), who showed that axial flow destabilizes SPF with respect to centrifugal instability from $Re = 0$ up to $Re \approx 13$. The critical Ta then rises slightly to a local maximum near $Re = 21$, before falling and reaching another minimum near $Re = 32$. Beyond that point, axial flow stabilizes SPF, with Ta_{crit} increasing monotonically until $Re \approx 200$. The scalloped nature of the stability boundary, corresponding to step changes in m_{crit}, is evident. The critical Ta

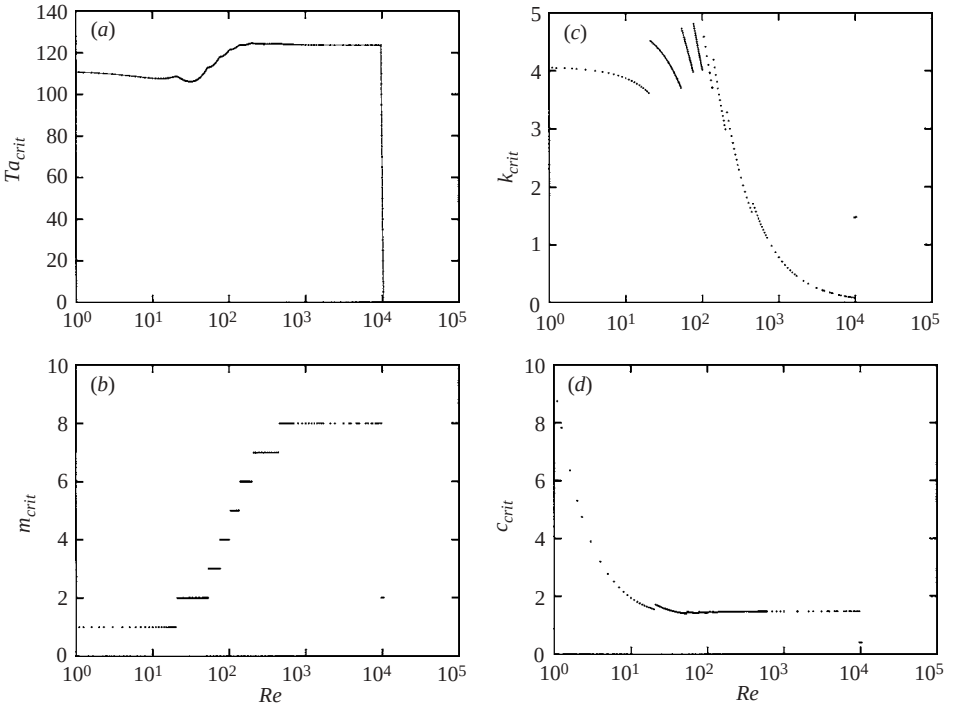

FIGURE 4. For $\mu = -0.5$ and $\eta = 0.5$: (*a*) critical *Ta*, (*b*) critical *m*, (*c*) critical *k*, (*d*) critical *c*, versus *Re*.

(≈ 124) remains approximately constant for $200 < Re < Re^* = 9683$, beyond which a precipitous drop occurs to $Ta = 0$ at Re_{AP}. The initial decrease of Ta_{crit} as *Re* increases from zero contrasts with the behaviour found for other μ. We note that there are values of *Ta* for which there exist up to three disjoint ranges of stable positive *Re* (discussed in § 5.5).

Figure 4(*b*) shows that m_{crit} again increases in unit steps with increasing *Re*, starting from 1 for $0 \leqslant Re < 20$ and increasing to 8 at Re^*. As for $\mu = 0.5$, there is again no *Re* for which $m_{crit} = 0$. As *Re* increases through Re^*, m_{crit} jumps directly from 8 to 2. For $Re^* \leqslant Re \leqslant Re_{AP}$, m_{crit} remains at 2.

As is the case for other values of μ, figure 4(*c*) shows that for $\mu = -0.5$, k_{crit} is again a piecewise-continuous function of *Re*. We find $\sigma_{i,crit} \neq 0$ and $m_{crit} = 1$ at $Re = 0$, corresponding to the counter-rotating Couette flow losing its stability to a non-axisymmetric time-periodic disturbance flow. Thus, as suggested by figure 4(*d*), c_{crit} becomes unbounded as $Re \to 0$. The critical frequency remains nearly constant over the *Re* range for which $m_{crit} = 1$, corresponding to c_{crit} being inversely proportional to *Re*. Subsequent increases in m_{crit} lead to progressively smaller jump increases in c_{crit}.

5. Discussion

5.1. *Dependence of the stability boundary on* μ

Figure 5 shows that at $Re = 0$, Ta_{crit} is higher for the co- and counter-rotating base states than for $\mu = 0$. (The $\mu = 0.5$ case, for which $\mu > \eta^2$, is linearly stable for all *Ta* at $Re = 0$.) Like the $\mu = 0.2$ case, for which $\mu = 0.8\eta^2$ is only 20% below the Rayleigh criterion, the $\mu = -0.5$ case is also stabilized, relative to $\mu = 0$, by outer-cylinder

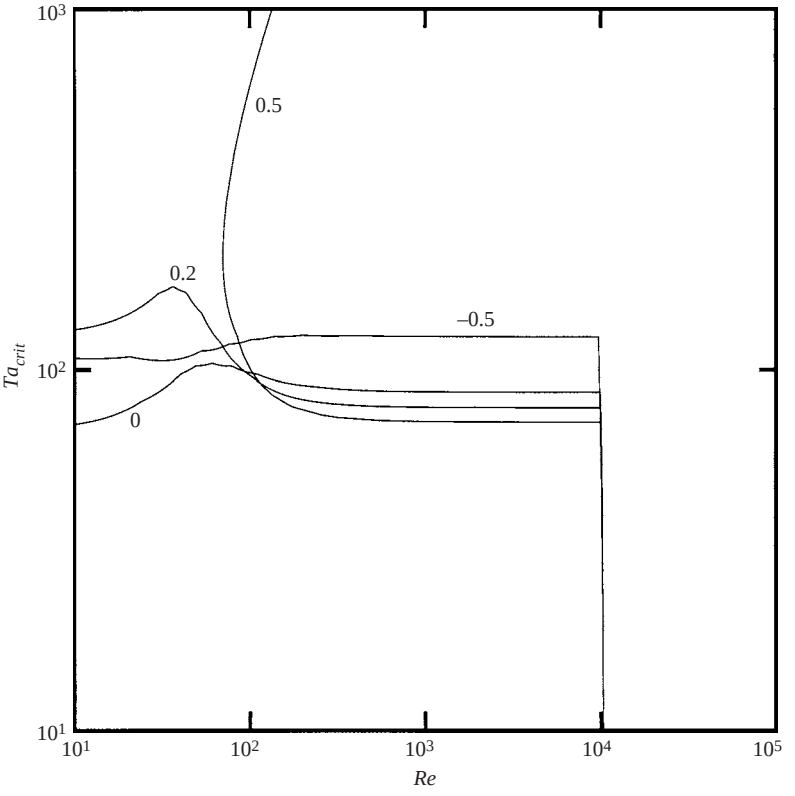

FIGURE 5. Critical *Ta* versus *Re* for $\eta = 0.5$ and $\mu = 0.5$, 0.2, 0, and -0.5.

rotation. As *Re* increases, the $\mu = 0.2$ co-rotating base flow becomes less stable than the $\mu = 0$ and -0.5 cases. For each $\mu < \eta^2$, Ta_{crit} approaches a nearly *Re*-independent value beyond about $Re = 500$ (with the lower branch of the multi-valued $\mu = 0.5$ stability boundary also approaching such a plateau). For the μ values considered, Ta_{crit} on the plateau decreases monotonically with increasing μ. At Re^* values depending very weakly on μ, centrifugal instability on the plateau ultimately gives way to a TS-like instability, with Ta_{crit} falling rapidly over $Re^* < Re < Re_{AP}$, where Re_{AP} is independent of μ.

For $\mu < \eta^2$, the stability boundary extends from $Re = 0$ to $Re = Re_{AP} = 10\,359$. For $\mu > \eta^2$, the stability boundary exists only for $Re_{min} \leqslant Re \leqslant Re_{AP}$, where we have shown (§ 4.2) that Re_{min} can be a turning point (for $\mu = 0.5$) or vertical asymptote (for $\mu = 1$). For $\mu = 1$, there is an asymptotic *Re* of about ~ 82.5 as $Ta \to \infty$ (Joseph & Munson 1970), consistent with our values of $Re_{crit} = 82.36$ and 82.33 at $Ta = 2000$ and 3000, respectively. Table 3 shows that differential rotation ($\mu \neq 1$) stabilizes SPF at high *Ta* for $\mu = 0.9$ and 1.2, and suggests that Re_{min} is a turning point for $\mu > \eta^2$, except when $\mu = 1$, in which case Re_{min} corresponds to a vertical asymptote.

5.2. *Comparison to previous work*

Except for the small differences identified in § 3, and attributed there to our slightly more stringent convergence criteria, our computed results for $\mu < \eta^2$ are essentially identical to those of Takeuchi & Jankowski (1981) over the *Re* range considered by them. Our results are very similar to their experimental data at low *Re*, and differ in

	μ		
Ta	0.9	1.0	1.2
300	80.74 (−8)	85.18 (−8)	92.33 (−6)
1000	86.31 (−6)	82.55 (−8)	132.9 (−5)
3000	144.2 (−5)	82.33 (−8)	264.0 (−5)

TABLE 3. Reynolds numbers on the stability boundary and azimuthal wavenumbers (in parentheses) for $\eta = 0.5$ and selected values of μ and Ta.

the higher part of their experimental range ($0 \leqslant Re \leqslant 150$) in the same way that their computations (for $0 \leqslant Re \leqslant 100$) differed from their own experiments. Also, as stated in § 3, comparison of our computed dimensionless drift velocity c_{crit} to the ratio ω_c/k_c of fitted functional forms computed by Recktenwald *et al.* (1993) for $0 \leqslant Re \leqslant 20$, $\mu = 0$, and $\eta = 0.5$ shows excellent agreement, with the r.m.s. error for $Re = 1, 2, \ldots, 20$ being 1.6×10^{-4}.

For $\mu = 0$, Meseguer & Marques (2002) reported results (their table 1 and figure 2) very close to the computations and experimental data of Takeuchi & Jankowski for small Re. For counter-rotating cylinders ($\mu < 0$), they stated that "When the cylinders are rotating with opposite signs of angular speeds, the centrifugal mechanism is dominant over the axial shear, as already concluded in Meseguer & Marques (2000), where the shear was induced by a relative sliding between the cylinders." As for $\mu = -0.5$ (figure 4*a*), there is in fact a transition from centrifugal to TS-like ('shear') instability at higher Re.

Consideration of an insufficient range of azimuthal wavenumbers, identified as the source of the discrepancy between our $\mu = 1$ results and those of Joseph & Munson (1970) on the one hand, and those of Meseguer & Marques (2002) on the other (see § 4.2), affects other stability boundaries reported by the latter authors. Their figure 4 shows a stability boundary in the (Re, Ta)-plane for $Re_{\theta,o} \equiv \Omega_o R_o (R_o - R_i)/\nu = 450$ (corresponding to $\mu Ta = 225$ for $\eta = 0.5$), beginning at $Re = 0$ just above $Ta = Re_{\theta,i} = 900$, with μ just below $\eta^2 = 0.25$. (Meseguer & Marques (2002) denoted these azimuthal Reynolds numbers by R_i and R_o.) For sufficiently large Re (say, $Re > 40$), Ta decreases monotonically, corresponding to increasing values of μ for $Re_{\theta,o}$ fixed. As one continues to smaller Ta on their stability boundary, one reaches a turning point near $Re = 107$, with Re now decreasing as Ta decreases. Near $Re = 103$, the stability boundary passes through $Ta = 450$, corresponding to $\mu = 0.5$. For $\mu = 0.5$, figure 4 of Meseguer & Marques (2002) shows SPF to be stable for Re up to about 103, with $m_{crit} = 5$ (their figures 4 and 10).

In contradistinction to those results, our computations for $\mu = 0.5$ show that the stability boundary passes through $Ta = 450$ near $Re = 86$ (see figure 2*a*), at which point $m_{crit} = -7$ (figure 2*b*). Over the range of Re considered by Meseguer & Marques (2002), our figure 6 shows the correct stability boundary in the (Re, Ta)-plane for $\mu Ta \equiv \eta Re_{\theta,o} = 225$ (corresponding to $Re_{\theta,o} = 450$ and their figure 4), along with the variation of m_{crit} along the curve. Results in figure 6 were obtained by selecting Ta, calculating μ from $\mu Ta = 225$, and then computing a critical Re, or by selecting Re, guessing a μ, computing the corresponding Ta_{crit}, and iterating on μ until $\mu Ta = 225$.

The correct stability boundary intersects the $Re = 0$ axis at two Ta_{crit} values, rather than at a single one shown by Meseguer & Marques (2002). The existence of critical values of Ta for both the co-rotating ($\mu > 0$, $Ta > 0$) and counter-rotating ($\mu < 0$,

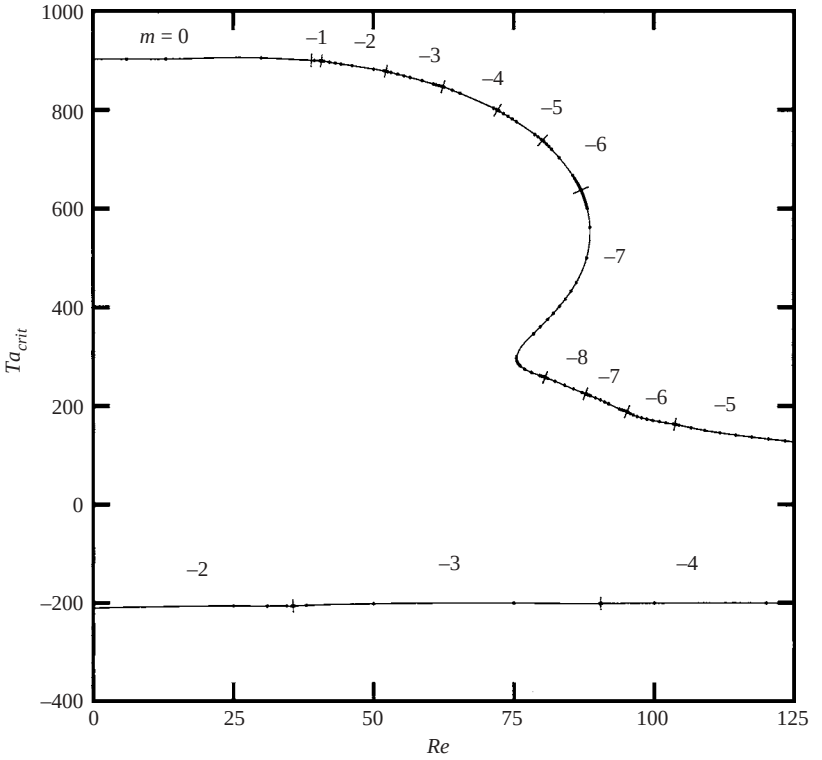

FIGURE 6. Critical Ta and m for $\eta = 0.5$ and $\mu Ta = 225$.

$Ta < 0$) cases for $\mu Ta = 225$ is consistent with $Re = 0$ results shown in figure 37.1.b of Joseph (1976). Steady axisymmetric SPF is stable in a region lying between the upper and lower portions of the stability boundary. We conjecture that the stability boundary crosses the $Ta = 0$ axis at $Re_{AP} = 10\,359$, with $\Omega_o(R_o - R_i)^2/\nu = \mu Ta$ maintaining its constant value of 225 while the sign of Ta (and Ω_i) changes. For $\mu Ta = 225$ and Re lying between the two turning points (at approximately 75 and 88), there are three disjoint ranges of $Ta = \Omega_i(R_o - R_i)^2/\nu$ for which SPF is unstable, and two in which SPF is linearly stable. At $Re = 0$, Ta_{crit} is invariant with respect to the sign of m, so that there is a positive critical azimuthal wavenumber, 2, in addition to the negative value shown. Also note that between $Re = 0$ and the point near $Re = 39.5$ at which $\mu = \eta^2 = 0.25$, Ta (and hence μ) is nearly constant, with Ta varying between 900 (near $Re = 39.5$) and about 905.3 (near $Re = 30$), and intersecting the $Re = 0$ axis near $Ta = 903.3$.

Comparison to figure 4 of Meseguer & Marques (2002) shows that even on the upper portion of the stability boundary, computed by them, the Re dependence of m_{crit} is entirely different. The reason is evident from our figure 3, which shows all neutral curves in the (k, Ta)-plane for $\mu = 0.5$ and $Re = 100$. In that case, SPF is stable below the minimum of the $m = 6$ neutral curve, and above the maximum of the $m = -7$ neutral curve (see also figure 2*b*). We conjecture that the results in figure 4 of Meseguer & Marques (2002) were obtained without considering $m < 0$, as for $\mu = 1$. When the correct asymptotic Re (82.36) is used in equation 5.9 of Meseguer & Marques (2002), the value of Re^{∞}_{eff} for SPF in their table 2 is reduced to 66.18, about 20% and 22% (rather than 7% and 9%) below the rotating Hagen–Poiseuille and

spiral Couette values (82.88 and 85.11) cited, respectively. The lower ($\mu < 0$) portion of the stability boundary in figure 6 shows that for $\Omega_o(R_o - R_i)^2/\nu = 225$, Ta_{crit} for the counter-rotating case is nearly independent of Re up to at least $Re = 125$.

We also note that the neutral curves shown in figure 5(*a–d*) of Meseguer & Marques (2002) are necessarily incomplete, since the critical azimuthal wavenumber shown on the middle ('hidden') branch of the stability boundary in their figure 4 is $m = 5$, whereas only the $m = 3$ and $m = 6$ neutral curves are shown in their figure 5(*a–d*) for Re values in the range of multiplicity. It is clear that disconnected neutral curves must exist for several values of m, as we have shown in figure 3 for $\mu = 0.5$ and $Re = 100$.

5.3. *Transition from centrifugal to Tollmien–Schlichting-like instability*

In his review of a paper by Chandrasekhar (1960), Reid (1961) conjectured that in the narrow-gap limit, the low-Re instability of SPF ultimately must connect to a TS-like instability at high Re. To date, such a connection has been made (for $\mu = 0$ and $\eta = 0.95$) only when disturbances are restricted to axisymmetric ones (Ng & Turner 1982).

For each μ considered, transition from centrifugal to TS-like instability occurs at Re^*, with a discontinuity in the slope of Ta versus Re. This is reminiscent of transition from Rayleigh–Bénard convection to TS waves in pressure-driven flow between horizontal plates heated from below (Gage & Reid 1968; Kelly 1994), where the mean flow has no effect on onset of Rayleigh–Bénard convection. For SPF, Re affects Ta_{crit} for onset of centrifugal instability (weakly on the plateau), and Ta affects the critical Re for TS-like instability (weakly). On the portion of the SPF stability boundary consisting of the plateau and the TS-like portion beyond, the similarity to plane Poiseuille flow heated from below is quite striking, with coupling between centrifugal and axial shear effects being very weak.

For each μ, m_{crit} decreases from its value on the high-Re plateau to 2 at Re^*. For $Re^* < Re \leqslant Re_{crit}$, $m_{crit} = 2$, so that we refer to instability in this range as 'Tollmien–Schlichting-like', since the 'true' TS instability (as $\eta \to 1$) is axisymmetric. The non-zero m_{crit} at Re_{AP} (for $\eta = 0.5$ and for $\eta > 0.5$, as shown in Part 2) is at variance with the expectation of an axisymmetric critical disturbance as Re approaches Re_{AP} (Ng & Turner 1982, p. 101). The critical axial wavenumber, k_{crit}, increases considerably as Re increases through Re^*.

5.4. *Multiple ranges of stable Ta for fixed Re*

For the multi-valued stability boundary found for $\mu = 0.5$, figure 2(*a*) shows that in some range of Re, SPF is linearly stable below the lower branch and above the upper branch, and unstable in between. The behaviour on the lower branch is similar to that predicted for $\mu < \eta^2$, with Ta_{crit} approaching a plateau value, and falling rapidly to zero between Re^* and Re_{AP}. On the upper branch, however, Ta_{crit} increases rapidly with Re. We interpret this as follows. For $\mu > \eta^2$, the Rayleigh criterion requires that circular Couette flow ($Re = 0$) is linearly stable for all Ta. Figure 2(*a*) shows that SPF is indeed stable for all Ta for $0 \leqslant Re < Re_{min}$, and is destabilized by axial shear in a progressively wider range of Ta as Re increases beyond Re_{min}. For $\mu = 0.5$, it is also apparent that for $Re > Re_{min}$, SPF can be destabilized by *decreasing* Ta across the upper branch of the stability boundary. For $\mu > \eta^2$ (and $\mu \neq 1$), it is unclear whether the upper branch exists for all $Re > Re_{min}$, or has a vertical asymptote at some finite Re.

In interpreting figure 2(*a*), note that crossing the two branches of the stability boundary at a single $Re > Re_{min}$ does not correspond to the same base flow becoming unstable at two different values of Ta. (This differs from cases cited in § 4.2, in which

multi-valued stability boundaries have been found for the same base state.) This is because, for fixed η, the magnitude of the azimuthal component of the base flow (2.1*b*) depends on Ta/Re, while the magnitude and profile of the axial component (2.1*c*) are invariant. Hence, we interpret the multi-valued stability boundary in figure 2(*a*) as meaning that SPF, with fixed profiles of the axial and azimuthal velocity components and a fixed magnitude of the axial component, is stable for two ranges of the magnitude of the azimuthal component and unstable in the intermediate range. Only if the boundary shown in figure 2(*a*) twice intersected a line $Ta = \alpha Re$ (α constant) could we state that the same base flow becomes unstable at two different Ta_{crit} values. We have found no such case.

We next consider experimental verification of the double-valued stability boundary predicted for $\mu = 0.5$. The existence of a multi-valued stability boundary for SPF is particularly significant, since SPF is one of only two steady isothermal flows for which multiple ranges of stability have been predicted, the other being spiral Couette flow (Meseguer & Marques 2000), for which the nominal base flow necessarily ceases to exist at a finite time (regardless of the Reynolds and Taylor numbers) for cylinders of finite length. (For the two-phase parallel shear flow considered by Blennerhassett (1980), the disconnected neutral curves shown (his figure 5) result from a two-dimensional linear stability analysis. As discussed by Pearlstein (1987) and Renardy (1989), Squire's transformation is applicable to that flow but Squire's theorem is not, so that the number of critical values of the Reynolds number cannot be determined on the basis of a two-dimensional analysis.) For no flow in which multi-valued stability boundaries have been predicted are we aware of experimental verification (or attempted verification) of the existence of multi-valued ranges of stability. From an experimental standpoint, a decided advantage of SPF, compared to doubly and multiply diffusive quiescent layers in which multiple ranges of stability have been predicted (Pearlstein 1981; Pearlstein *et al.* 1989; Terrones & Pearlstein 1989; Lopez *et al.* 1990), is that SPF does not require establishment and maintenance of one or more concentration gradients, which is difficult in systems with the rigid impermeable boundaries used in the analyses.

To locate two values of Ta_{crit} at fixed Re beyond the turning point at Re_{min}, a simple approach is to start at two Ta values (with the same μ), greater than and less than $Ta(Re_{min})$, and to increase Re from zero, where circular Couette flow is stable according to the Rayleigh criterion. If for both Ta one can proceed to an $Re > Re_{min}$ without destabilizing the base flow, one can then stop at that Re, and increase the smaller Ta and decrease the larger Ta, until both branches of the stability boundary are located. If there is no Ta pair bracketing $Ta(Re_{min})$ for which it is possible to maintain the base flow from $Re = 0$ to $Re > Re_{min}$, then one must conclude that finite-amplitude instability occurs along the path(s) chosen.

5.5. *Multiple ranges of stable Re for fixed Ta*

Multiplicity results related to those discussed in § 5.4 are apparent in the work of Takeuchi & Jankowski, whose figure 1(*a*) shows that for $\mu = 0$, Ta passes through a local maximum near $Re = 60$, corresponding to existence of multiple critical values of Re over some Ta range. For $\mu = 0$, our figure 1(*a*) shows that for each Ta in the range $68.19 < Ta < 104.4$, SPF is stable over a finite Re range not including $Re = 0$. For $Ta = 100$, figure 7 shows that the stable Re range lies between the minimum of a 'banana-shaped' $m = 5$ neutral curve, and the maximum of a closed and disconnected $m = 2$ neutral curve. The other neutral curves shown ($m = 0$ and 1) pass through the $Re = 0$ axis. Since the instability mechanism must be independent of axial and

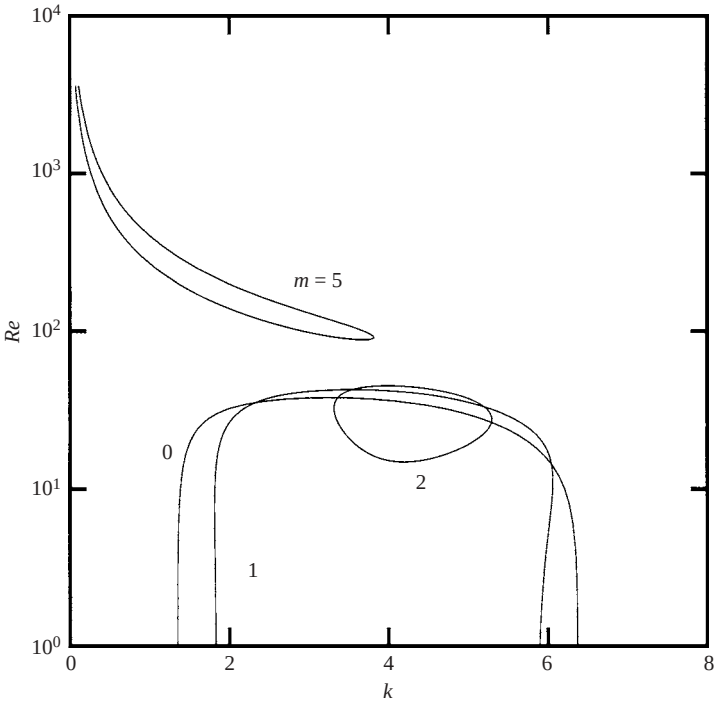

FIGURE 7. Neutral curves for $Ta = 100$, $\mu = 0$, and $\eta = 0.5$.

azimuthal flow directions, each neutral curve must be symmetric about the $Re = 0$ axis, from which it follows that in the $k \geqslant 0$ half of the (k, Re)-plane, the $m = 0$ and $m = 1$ neutral curves are closed.

Invariance of the instability mechanism with respect to the directions of cylinder rotation and axial flow can be used to represent the stability boundary in the full (Re, Ta)-plane instead of its positive quadrant. For $\mu = 0$, Ta_{crit} is a unimodal function of Re for $Re \geqslant 0$, and figure 1(a) shows that for sufficiently small Ta, SPF is linearly stable over $0 \leqslant Re \leqslant Re_{TS}(Ta)$, where Re_{TS} is the critical Re for TS-like instability between Re^* and Re_{AP}, and $Re_{TS}(0) = Re_{AP}$. For $\mu = 0$ and $|Ta| \leqslant Ta_1 = 68.19$, it follows from figure 1(a) that SPF is linearly stable for $-Re_{TS}(Ta) \leqslant Re \leqslant Re_{TS}(Ta)$, while for $|Ta| > Ta_2 = 104.4$ there is no stable Re range. In each intermediate Ta range, $-Ta_2 \leqslant Ta \leqslant -Ta_1$ and $Ta_1 \leqslant Ta \leqslant Ta_2$, there are two disjoint finite ranges of stable Re, corresponding to gaps between the primary neutral curves and the extrema of disconnected neutral curves lying between them in the (k, Ta)-plane. One, for positive Re, was discussed in the previous paragraph. The other, for negative Re, is its mirror image.

Figure 4(a) shows that for $\mu = -0.5$, Ta_{crit} is not a unimodal function of Re. When viewed in terms of a critical Ta versus Re in the positive quadrant of the (Re, Ta)-plane, the stability boundary is single-valued, and there are no closed disconnected neutral curves in the (k, Ta)-plane at fixed Re. On the other hand, figure 4(a) shows that there can be one, three, or five positive critical Re for fixed Ta (at, e.g., $Ta = 105$, 107, and 108, respectively). Multiple critical Re at fixed Ta must correspond to existence of one or more closed disconnected neutral curves in the (k, Re)-plane, each with at least two extrema.

5.6. *Direction of wave propagation*

For all cases considered other than $\mu = 0.5$, we have $m_{crit} \geqslant 0$ and $c_{crit} > 0$ over the entire range of Re, and disturbances propagate downstream with the base flow, with the same helical sense. For $\mu = 0.5$, however, figures 2(*b*) and 2(*d*) show that on the upper branch, m_{crit} and c_{crit} are negative. Thus, for $\mu = 0.5$, linear theory predicts that as Ta increases and crosses the upper branch of the stability boundary, or decreases through the lower branch sufficiently close to the turning point, SPF becomes unstable with respect to a disturbance propagating upstream against the mean axial flow, but with the same helical sense as the base flow. Figure 2(*d*) shows that c_{crit} changes sign discontinuously on the lower branch at the transition from $m_{crit} = 6$ to -6 near the turning point, and is non-zero on the entire stability boundary.

6. Conclusions

For $\eta = 0.5$, the complete linear stability boundaries for spiral Poiseuille flow presented in § 4 show that for each rotation rate ratio $\mu < \eta^2$ considered, we can connect the onset of instability for circular Couette flow with no mean axial flow to the onset of instability in annular Poiseuille flow without rotation. For $\mu > \eta^2$, SPF is linearly stable for $0 \leqslant Re < Re_{min}$. For $\mu > \eta^2$ and $\mu \neq 1$, there is a turning point at Re_{min}, beyond which there exists a range of Re for which the stability boundary is multi-valued and there are two disjoint ranges of stable Ta. For the special case $\mu = 1$, there is a vertical asymptote in the (Re, Ta)-plane at $Re_{min} = 82.33$, a value differing from that found by Meseguer & Marques (2002), apparently due to consideration of an insufficient range of the azimuthal wavenumber m.

For $\mu < \eta^2$, a small mean axial pressure gradient generally stabilizes SPF with respect to centrifugal instability, as shown by earlier investigators. In each case, Ta_{crit} reaches a plateau before falling precipitously to zero as Re approaches Re_{AP}, the critical Reynolds number for annular Poiseuille flow. Transition from centrifugal instability at small Re to a shear instability of Tollmien–Schlichting type occurs at Re^* (slightly below Re_{AP}), at which m_{crit} drops from its value on the high-Re plateau to 2.

We acknowledge helpful comments by Professor Howard A. Snyder and anonymous reviewers. This work was supported in part by NSF Grants CTS-9422770 and CTS-9613241, and DOE Grant DE-FG02-96ER45607. Some of the computations were performed using the facilities of the National Center for Supercomputing Applications.

REFERENCES

Ali, M. & Weidman, P. D. 1990 On the stability of circular Couette flow with radial heating. *J. Fluid Mech.* **220**, 53–84.

Babcock, K. L., Ahlers, G. & Cannell, D. S. 1991 Noise-sustained structure in Taylor–Couette flow with through flow. *Phys. Rev. Lett.* **67**, 3388–3391.

Babcock, K. L., Ahlers, G. & Cannell, D. S. 1994 Noise amplification in open Taylor–Couette flow. *Phys. Rev.* E **50**, 3670–3692.

Babcock, K. L., Cannell, D. S. & Ahlers, G. 1992 Stability and noise in Taylor–Couette flow with through-flow. *Physica* D **61**, 40–46.

Blennerhassett, P. J. 1980 On the generation of waves by wind. *Phil. Trans. R. Soc. Lond.* A **298**, 451–494.

Büchel, P., Lücke, M., Roth, D. & Schmitz, R. 1996 Pattern selection in the absolutely unstable regime as a nonlinear eigenvalue problem: Taylor vortices in axial flow. *Phys. Rev.* E **53**, 4764–4777.

Bühler, K. & Polifke, N. 1990 Dynamical behaviour of Taylor vortices with superimposed axial flow. In *Nonlinear Evolution of Spatio-Temporal Structures in Dissipative Continuous Systems* (ed. F. H. Busse & L. Kramer), pp. 21–29. Plenum.

Chandrasekhar, S. 1960 The hydrodynamic stability of viscid flow between coaxial cylinders. *Proc. Natl Acad. Sci. USA* **46**, 141–143.

Cornish, R. J. 1933 Flow of water through fine clearances with relative motion of the boundaries. *Proc. R. Soc. Lond.* A **140**, 227–240.

Cotrell, D. L., Rani, S. L. & Pearlstein, A. J. 2004 Computational assessment of subcritical and delayed onset in spiral Poiseuille flow experiments. *J. Fluid Mech.* **509**, 353–378 (referred to herein as Part 2).

DiPrima, R. C. & Swinney, H. L. 1985 Instabilities and transition in flow between concentric rotating cylinders. In *Hydrodynamic Instabilities and the Transition to Turbulence* (ed. H. L. Swinney & J. P. Gollub), 2nd edn, pp. 139–180. Springer.

Gage, K. S. & Reid, W. H. 1968 The stability of thermally stratified plane Poiseuille flow. *J. Fluid Mech.* **33**, 21–32.

Garg, V. K. 1980 Spatial stability of concentric annular flow. *J. Phys. Soc. Japan* **49**, 1577–1583.

Goldstein, S. 1937 The stability of viscous fluid flow between rotating cylinders. *Proc. Camb. Phil. Soc.* **33**, 41–61.

Hu, H.-C. & Kelly, R. E. 1995 Effect of a time-periodic axial shear flow upon the onset of Taylor vortices. *Phys. Rev.* E **51**, 3242–3251.

Johnson, E. C. & Lueptow, R. M. 1997 Hydrodynamic stability of flow between rotating porous cylinders with radial and axial flow. *Phys. Fluids* **9**, 3687–3696.

Joseph, D. D. 1976 *Stability of Fluid Motions I*. Springer.

Joseph, D. D. & Munson, B. R. 1970 Global stability of spiral flow. *J. Fluid Mech.* **43**, 545–575.

Kelly, R. E. 1994 The onset and development of thermal convection in fully developed shear flows. *Adv. Appl. Mech.* **31**, 35–112.

Kolyshkin, A. A. & Vaillancourt, R. 1997 Convective instability boundary of Couette flow between rotating porous cylinders with axial and radial flows. *Phys. Fluids* **9**, 910–918.

Lopez, A. R., Romero, L. A. & Pearlstein, A. J. 1990 Effect of rigid boundaries on the onset of convective instability in a triply diffusive fluid layer. *Phys. Fluids* A **2**, 897–902.

Lücke, M. & Recktenwald, A. 1993 Amplification of molecular fluctuations into macroscopic vortices by convection instabilities. *Europhys. Lett.* **22**, 559–564.

Lueptow, R. M., Docter, A. & Min, K. 1992 Stability of axial flow in an annulus with a rotating inner cylinder. *Phys. Fluids* A **4**, 2446–2455.

Mahadevan, R. & Lilley, G. M. 1977 The stability of axial flow between concentric cylinders to asymmetric disturbances. *AGARD* CP-224, pp. 9-1–9-10.

Marques, F. & Lopez, J. M. 2000 Spatial and temporal resonances in a periodically forced hydrodynamic system. *Physica* D **136**, 340–352.

Mavec, J. A. 1973 Spiral and toroidal secondary motions in swirling flows through an annulus at low Reynolds numbers. MS Thesis, Illinois Inst. Tech., Chicago.

Meseguer, A. & Marques, F. 2000 On the competition between centrifugal and shear instability in spiral Couette flow. *J. Fluid Mech.* **402**, 33–56.

Meseguer, A. & Marques, F. 2002 On the competition between centrifugal and shear instability in spiral Poiseuille flow. *J. Fluid Mech.* **455**, 129–148.

Min, K. & Lueptow, R. M. 1994 Circular Couette flow with pressure-driven axial flow and a porous inner cylinder. *Exps. Fluids* **17**, 190–197.

Moser, K. W., Raguin, L. G. & Georgiadis, J. G. 2001 Tomographic study of helical modes in bifurcating Taylor–Couette–Poiseuille flow using magnetic resonance imaging. *Phys. Rev.* E **64**, 016319.

Moser, K. W., Raguin, L. G., Harris, A., Morris, H. D., Georgiadis, J., Shannon, M. & Philpott, M. 2000 Visualization of Taylor–Couette and spiral Poiseuille flows using a snapshot FLASH spatial tagging sequence. *Magn. Reson. Imaging* **18**, 199–207.

Nagib, H. M. 1972 On instabilities and secondary motions in swirling flows through annuli. PhD Dissertation, Illinois Inst. Tech., Chicago.

Ng, B. S. & Turner, E. R. 1982 On the linear stability of spiral flow between rotating cylinders. *Proc. R. Soc. Lond.* A **382**, 83–102.

Pearlstein, A. J. 1981 Effect of rotation on the stability of a doubly diffusive fluid layer. *J. Fluid Mech.* **103**, 389–412.

Pearlstein, A. J. 1987 The onset of stability via three-dimensional disturbances in parallel shear flows. *Bull. Am. Phys. Soc.* **32**, 2087.

Pearlstein, A. J., Harris, R. M. & Terrones, G. 1989 The onset of convective instability in a triply diffusive fluid layer. *J. Fluid Mech.* **202**, 443–465.

Pinter, A., Lücke, M. & Hoffmann, Ch. 2003 Spiral and Taylor vortex fronts and pulses in axial through flow. *Phys. Rev.* E **67**, 026318.

Raffaï, R. & Laure, P. 1993 The influence of an axial mean flow on the Couette–Taylor problem. *Eur. J. Mech.* B/*Fluids* **12**, 277–288.

Recktenwald, A., Lücke, M. & Müller, H. W. 1993 Taylor vortex formation in axial through-flow: Linear and weakly nonlinear analysis. *Phys. Rev.* E **48**, 4444–4454.

Reid, W. H. 1961 Review of "The hydrodynamic stability of viscid flow between coaxial cylinders" by S. Chandrasekhar (*Proc. Natl Acad. Sci. USA* **46**, 141–143, 1960). *Math. Rev.* **22**, 565.

Renardy, Y. 1989 Weakly nonlinear behavior of periodic disturbances in two-layer Couette–Poiseuille flow. *Phys. Fluids* A **1**, 1666–1676.

Sadeghi, V. M. & Higgins, B. G. 1991 Stability of sliding Couette–Poiseuille flow in an annulus subject to axisymmetric and asymmetric disturbances. *Phys. Fluids* A **3**, 2092–2104.

Snyder, H. A. 1962 Experiments on the stability of spiral flow at low axial Reynolds numbers. *Proc. R. Soc. Lond.* A **265**, 198–214.

Snyder, H. A. 1965 Experiments on the stability of two types of spiral flow. *Ann. Phys.* **31**, 292–313.

Swift, J. B., Babcock, K. L. & Hohenberg, P. C. 1994 Effects of thermal noise in Taylor–Couette flow with corotation and axial through-flow. *Physica* A **204**, 625–649.

Synge, J. L. 1938 On the stability of a viscous liquid between two rotating coaxial cylinders. *Proc. R. Soc. Lond.* A **167**, 250–256.

Takeuchi, D. I. & Jankowski, D. F. 1981 A numerical and experimental investigation of the stability of spiral Poiseuille flow. *J. Fluid Mech.* **102**, 101–126, and corrigendum **113**, 536 (1981).

Taylor, G. I. 1923 Stability of a viscous liquid contained between two rotating cylinders. *Phil. Trans. R. Soc. Lond.* A **223**, 289–343.

Terrones, G. & Pearlstein, A. J. 1989 The onset of convection in a multicomponent fluid layer. *Phys. Fluids* A **1**, 845–853.

Tsameret, A., Goldner, G. & Steinberg, V. 1994 Experimental evaluation of the intrinsic noise in the Couette–Taylor system with an axial flow. *Phys. Rev.* E **49**, 1309–1319.

Tsameret, A. & Steinberg, V. 1991*a* Convective *vs.* absolute instability in Couette–Taylor flow with an axial flow. *Europhys. Lett.* **14**, 331–336.

Tsameret, A. & Steinberg, V. 1991*b* Noise-modulated propagating pattern in a convectively unstable system. *Phys. Rev. Lett.* **67**, 3392–3395.

Tsameret, A. & Steinberg, V. 1994*a* Absolute and convective instabilities and noise-sustained structures in the Couette–Taylor system with an axial flow. *Phys. Rev.* E **49**, 1291–1308.

Tsameret, A. & Steinberg, V. 1994*b* Competing states in a Couette–Taylor system with an axial flow. *Phys. Rev.* E **49**, 4077–4086.

Weisberg, A. Y., Kevrekidis, I. G. & Smits, A. J. 1997 Delaying transition in Taylor–Couette flow with axial motion of the inner cylinder. *J. Fluid Mech.* **348**, 141–151.

Wereley, S. T. & Lueptow, R. M. 1999 Velocity field for Taylor–Couette flow with an axial flow. *Phys. Fluids* **11**, 3637–3649.